Reconfiguration of interdomain communication in hexokinase 1: A molecular basis for NEDVIBA childhood neurodevelopmental disorder SUPPLEMENTARY MATERIAL

Alberto Galli[1], **Giovanni La Penna**[2,3,*,+], **Germano Nobili**[4], **and Silvia Rinaldi**[2,*,+]

[1]Independent scholar
[2]Institute of chemistry of organometallic compounds, National research council
[3]Roma-Tor Vergata section, National Institute for Nuclear Physics
[4]Department of physics, University of Roma Tor Vergata
[*]giovanni.lapenna@cnr.it, silvia.rinaldi@cnr.it
[+]These authors contributed equally to this work

ABSTRACT

This Supplementary material contains figures and tables that are useful to understand the applied methods, while being marginal information to understand results.

Results

Stability of helix-a13 region

In Fig. S1 we display two configurations contributing to the statistics providing different values of ξ. On the right panel the

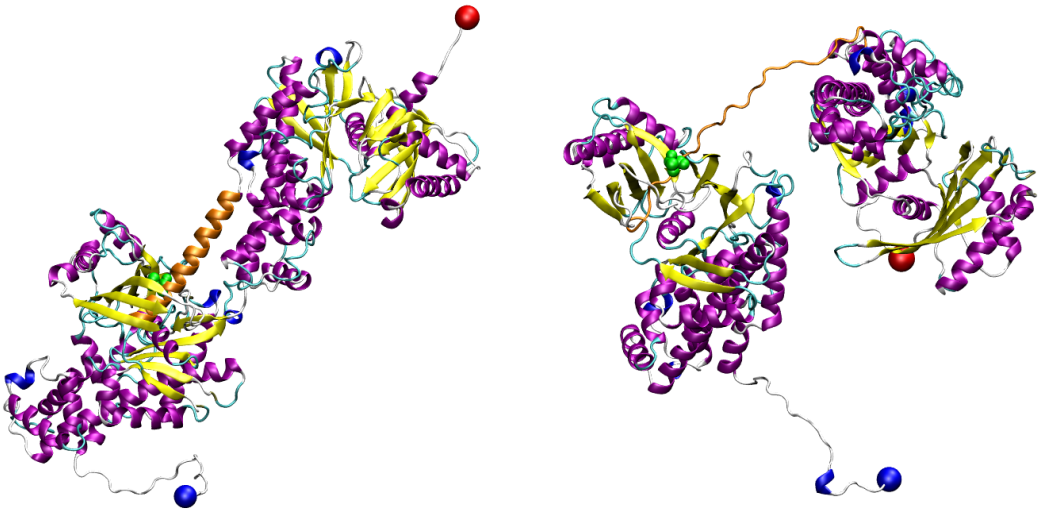

ξ =21
RMSD(Nd)=2.3 Å
RMSD(Cd)=2.1 Å

ξ =3
RMSD(Nd)=3.9 Å
RMSD(Cd)=4.3 Å

Figure S1. Two sampled configurations with maximal (left) and minimal (right), respectively, α-helix content in region helix-a13. The variable ξ is the number of α-helical backbone hydrogen-bonds in region 450-477. RMSD(Nd) and RMSD(Cd) are the root-mean square deviation (Å) of C, N, Cα and O atoms using aligned residues in N-terminal (Nd) and C-terminal (Cd) domains of HK4. Thr 457 in WT sequence is displayed in green spheres. N- and C-termini are displayed as a blue sphere (bottom-left) and red sphere (top-right), respectively. The backbone of region helix-a13 is displayed in orange. The STRIDE[1] method was used to represent helical (purple and blue), β-strands (yellow), turns (cyano) and loops (white). The VMD[2] program was used for molecular drawings.

configuration displays low order in the helix-a13 region, clearly shown by the flexibility of the orange ribbon between the two domains. Conversely, on the left panel the high order of the same region is shown by the long α-helical segment (in orange). The more evident flexibility of region helix-a13 when ξ is lower allows a significant displacement of the C-terminal domain (top of each panel) with respect to the N-terminal domain (bottom).

T457M alters the inter-domain interactions

In Table 1 the ratio between inertia momenta about the long axis (1) and the two short axes (2 and 3) are reported, as they are measured in metastatistics.

Variant	Nd		Cd	
	I_1/I_2	I_1/I_3	I_1/I_2	I_1/I_3
WT	0.64 (0.06)	0.55 (0.04)	0.66 (0.05)	0.56 (0.03)
T457M	0.64 (0.05)	0.55 (0.03)	0.65 (0.04)	0.56 (0.02)

Table S1. Inertia anisotropies for WT and T457M HK1 variant in N-terminal (middle columns) and C-terminal (right columns) domains. Inertia momenta are ordered from the smallest (1) to the largest (3) eigenvalues. Averages and root-mean square deviations (in brackets) are computed in the metastatistics.

Methods

Metadynamics

Simulation stages are summarised in Table S2.

Simulation Stage	Ensemble	Bias	α	w	t (ns)
0	NVT	–	–	–	0.4
1	NPT	–	–	–	4
2	NPT	+	0.00	1	2
3	NPT	+	0.25	1	2
4	NPT	+	0.50	1	2
5	NPT	+	0.75	1	2
6	NPT	+	1.00	0.5	2
7	NPT	+	–	–	2
8	NPT	–	–	–	2×500

Table S2. Parameters used in MD simulation for each walker. Temperature T is 300 K, except in stage 0 where it is step-wise increased from 50 to 300 K during the first 0.4 ns. The NPT ensemble, with the pressure P kept constant at 1 bar, was used. Wherever the values of α and w are reported, these numbers are used to implement Eq. 3 of Ref. 3. The bias used at the each stage (when + symbol is present) is obtained as a combination of the biases coming from all the walkers determined in the previous stage. In the last stage (7) the bias is no more updated with deposited gaussian functions. Sampling performed in stage 7 for all walkers provides the metastatistics that will be modulated (see Sect. "Free energy change" in Methods of main article). Sampling performed in stage 8 for walkers 1 (WT and T457M sequences) provides the isothermal/isobaric ensemble for the analysis of distance fluctuations and energy decomposition matrix.

Free energy change

The last two terms in Eq. 3 (main text) represent solute-solvent contributions to free energy at fixed Q. Some of the details to compute these terms are in the following.

The term $G_{solv,np}$ is the contribution to the solute-solvent free energy due to the formation of a cavity of zero charge density with the shape of the solute protein and the creation of the solute-solvent interface. Introducing a charge density in the space occupied by the solute leads to the $G_{solv,pol}$ contribution. The charge density is given in terms of the point charges q_i of the atom i sitting at the point $\vec{r}_i$, where i runs over the N_a atoms of the solute molecule.

The term $G_{solv,np}$ is calculated as an empirical linear combination of the solvent accessible surface area (SASA) for each group in the solute molecule[4] according to the formula

$$G_{solv,np} = \sum_{i}^{N_a} \sigma_i SASA_i \ , \tag{1}$$

where the coefficients σ_i are positive or negative for hydrophobic or hydrophilic groups, respectively. Finally the electrostatic contribution to the solute-solvent free energy, $G_{solv,pol}$, is given by the electrostatic energy required to charge the low-dielectric solute molecule of generic shape into a high-dielectric medium like a salt-water solution. The magnitude of this contribution is obtained by a numerical finite difference solution of the Poisson–Boltzmann equation[5]. The dielectric permittivity was 1 inside the surface and 80 outside. The radius of the probe used to measure the solvent-accessible surface area was 1.4 Å and the algorithm to compute the surface was the same used by GROMACS[6].

References

1. Frishman, D. & Argos, P. Knowledge-based secondary structure assignment. *Proteins: Struct., Func. & Genet.* **23**, 566–579, DOI: 10.1002/prot.340230412 (1995).

2. Humphrey, W., Dalke, A. & Schulten, K. VMD visual molecular dynamics. *J. Molec. Graph.* **14**, 33–38, DOI: 10.1016/0263-7855(96)00018-5 (1996). Http://www.ks.uiuc.edu/Research/vmd.

3. Hošek, P., Kříž, P., Toulcová, D. & Spiwok, V. Multisystem altruistic metadynamics- well-tempered variant. *J. Chem. Phys.* **146**, 125103, DOI: 10.1063/1.4978939 (2017).

4. Ooi, T., Oobatake, M., Némethy, G. & Scheraga, H. A. Accessible surface areas as a measure of the thermodynamic parameters of hydration of peptides. *Proc. Natl. Acad. Sci.* **84**, 3086–3090, DOI: 10.1073/pnas.84.10.3086 (1987).

5. Rocchia, W. *et al.* Rapid grid-based construction of the molecular surface and the use of induced surface charge to calculate reacton field energies: Applications to the molecular systems and geometric objects. *J. Comput. Chem.* **23**, 128–137, DOI: 10.1002/jcc.1161 (2002).

6. Eisenhaber, F., Lijnzaad, P., Argos, P., Sander, C. & Scharf, M. The double cubic lattice method: Efficient approaches to numerical integration of surface area and volume and to dot surface contouring of molecular assemblies. *J. Comput. Chem.* **16**, 273–284, DOI: 10.1002/jcc.540160303 (1995).